

## CYLINDER VIBRATION EXCITED BY SHEAR LAYERS FROM AN UPSTREAM CYLINDER

Md. Mahbub Alam and Y. Zhou

Department of Mechanical Engineering,  
 The Hong Kong Polytechnic University  
 Hung Hum, Kowloon, Hong Kong,  
 mmalam@polyu.edu.hk, mmyzhou@polyu.edu.hk

### ABSTRACT

This paper presents the free vibration of a cantilever-supported circular cylinder of diameter  $D$  placed behind another of smaller diameter  $d$ . The diameter ratio  $d/D$  is  $0.24 \sim 1.00$  and cylinder spacing  $L/d$  is  $1 \sim 2$ , where  $L$  is distance between the centre of the upstream cylinder to the forward stagnation point of the downstream cylinder. In this range of  $L/d$ , the shear layers separating from the upstream cylinder reattach on the downstream cylinder. An unusual violent vibration was observed at  $d/D = 0.24 \sim 0.8$  for  $L/d = 1$  or  $d/D = 0.24 \sim 0.6$  for  $L/d = 2$ , but not at  $d/D = 1$ . It is proposed that, at a small  $d/D$ , the upstream cylinder wake narrows, and the shear-layer reattachment position on the downstream cylinder approaches the forward stagnation point, and hence the high-speed slice of the shear layer could impinge upon alternately the two sides of the cylinder, thus exciting the downstream cylinder. The violent vibration occurs at a reduced velocity  $U_r (= U_\infty D/f_n)$ , where  $U_\infty$  is the free-stream velocity and  $f_n$  is the natural frequency of the fluid-structure system associated with the downstream cylinder)  $\approx 13\sim 22.5$ , depending on  $d/D$  and  $L/d$ , and grows rapidly, along with the fluctuating lift, for a higher  $U_r$ . To our knowledge, this phenomenon has not been reported previously and may have important implication in engineering applications. It is further noted that the flow behind the downstream cylinder is characterized by two predominant frequencies, corresponding to the cylinder vibration frequency and the natural frequency of vortex shedding from the downstream cylinder, respectively. While the former persists downstream, the latter vanishes rapidly.

### INTRODUCTION

Non-linear interaction between flow around and elastic behavior of a structure may generate a high magnitude of fluctuating forces and vibration. Most structures on land and in the ocean are in multiple forms, such as groups of chimney stacks, tubes in heat exchangers, overhead power-line bundles, bridge piers, stays, masts, chemical reaction towers, off-shore platforms, adjacent skyscrapers, etc. Fluid-flow interaction on the multiple structures is very complex. Flow-induced forces, elastic response, Strouhal frequencies and flow structure generated are major parameters considered for the aerodynamic design of the structures. Thus the study of these parameters of two closely separated cylinders is of both fundamental and practical significance.

Bokaian & Geoola (1984a) investigated the case of two identical cylinders where the upstream cylinder is fixed and the downstream one is both-end-spring-mounted, allowing

both ends to vibrate at the same amplitude (i.e., two-dimensional model) and in the cross-flow direction only. The investigated ranges of spacing ratio between the cylinders  $L/d$ , reduced velocity  $U_r (= U_\infty D/f_n)$  and Reynolds number  $Re (= U_\infty D/\nu)$  were  $0.59\sim 4.5$ ,  $3.8\sim 10$ ,  $600\sim 6000$ , where  $U_\infty$  is the free-stream velocity,  $\nu$  is kinematic viscosity of fluid, and  $f_n$  is natural frequency of the cylinder system; see Fig. 1 for the definitions of  $d$ ,  $D$  and  $L$ . Depending on  $L/d$ , the cylinder exhibited only galloping ( $L/d = 0.59$ ), or only vortex resonance ( $L/d > 2.5$ ) or a combined vortex-resonance and galloping ( $L/d = 1.0$ ), or a separated vortex excitation (VE) and galloping ( $1.5 \leq L/d \leq 2.5$ ). Bokaian & Geoola (1984b) almost at the same  $L/d$ ,  $U_r$  and  $Re$  ranges investigated the other case where the downstream cylinder is fixed and the upstream one is both-end-spring-mounted. They reported both galloping and vortex-resonance vibration generated for  $L/d \leq 1.25$  and  $1.25 < L/d < 4.5$ , respectively. For both VE and galloping, vortex shedding frequency  $f_v$  was found to lock-on to vibration frequency. Note that the vibration always occurs at  $f_n$ . The VE corresponds to vibration occurring near  $U_r$  where the natural vortex shedding frequency is close to  $f_n$ , and the galloping vibrations persist for higher  $U_r$ , corresponding to a

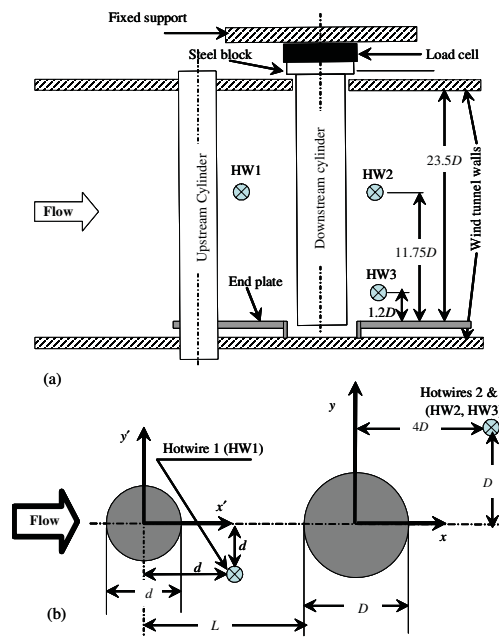


Fig. 1. (a) Experimental set-up, (b) definition of symbols

higher natural vortex shedding frequency than  $f_n$ . The mass-damping parameter  $m^*\zeta$  was 0.018–0.2, where  $m^*$  is the mass ratio and  $\zeta$  is the damping ratio. Brika and Laneville (1997, 1999) investigated response of the downstream cylinder with the upstream cylinder stationary or vibrating, for  $L/d = 6.5 \sim 24.5$ ,  $U_r = 4 \sim 21$  ( $Re = 5.1 \times 10^3 \sim 2.75 \times 10^4$ ). The system had a very low  $m^*\zeta$  of 0.00007. When the upstream cylinder was stationary, the response of the downstream cylinder was no more hysteretic and it was strongly dependent on  $L/d$ ; VE regime became wider and shifted to lower  $U_r$ , with increasing  $L/d$ . For  $L/d = 6.5 \sim 8$ , the cylinder exhibited a combination of VE and galloping. Hover & Triantafyllou (2001) examined response of and forces on the spring-mounted downstream cylinder for  $L/d = 4.25$ . They observed both VE and galloping to occur when  $U_r$  was varied from 2 to 17, with changing  $f_n$  at constant  $U_\infty$  corresponding to  $Re = 3.05 \times 10^4$ . Time-averaged drag coefficient ( $C_D$ ), and fluctuating drag coefficient ( $C_{Drms}$ ) were remarked to increase by about two times in the vortex-resonance and galloping regimes, but fluctuating lift ( $C_{Lrms}$ ) increased in VE regime and decreased with  $U_r$  in galloping regime. There are some other studies concerning flow-induced forces on two tandem fixed cylinders (e.g., Alam et al. 2003; Zdravkovich and Pridden 1977) and flow characteristics over the two cylinders vibrated forcibly in in-phase and out-of-phase modes (e.g., Mahir and Rockwell 1996). A detail survey of research relating to flow-induced response of tandem cylinders suggest that previous investigations mostly were performed for (i) two cylinders of an identical diameter, (ii) two-dimensional model (spring mounted at both ends), (iii) single degree of freedom (either cross-flow or streamwise), and (iv) at a low  $m^*\zeta$  value. The literatures mainly clarified  $L/d$  range where vortex-resonance or galloping persists. There does not seem to have a systematic study on flow-induced response of the downstream cylinder when upstream cylinder size (diameter) is changed.

The above mentioned points raise a number of questions. Firstly, what is the effect of upstream cylinder diameter on flow-induced response of the downstream cylinder? Secondly, what would be the response of the cylinder if it is cantilever mounted where the vibration amplitude is dependent on spawise location of the cylinder, three-dimensional model? Thirdly, is galloping or VE generated for a high value of  $m^*\zeta$ ? Fourthly, how much forces on the structure base are induced when a structure experiences VE or galloping? Finally, what is the physics behind the generation of galloping for tandem cylinders, though galloping in general is not generated on an isolated circular cylinder (axis-symmetric body)?

This work aims to study experimentally flow-induced response of a cantilever circular cylinder at a high  $m^*\zeta$  ( $=3.95$ ) value in the presence of an upstream cylinder of different diameters. The free end of the cantilever cylinder is free to move in two degrees of freedom. The upstream cylinder diameter ( $d$ ) is varied, with the downstream cylinder diameter ( $D$ ) unchanged, so that the ratio  $d/D$  varies from 1.0 to 0.24. Two  $L/d = 1.0$  and 2.0 are considered, and they are within the reattachment regime. The flow-induced responses  $A_x$  and  $A_y$  in the  $x$ - and  $y$ -direction (where  $A$  stands for amplitude of vibration at the free-end of the cylinder), forces on the cylinder base  $C_D$ ,  $C_{Drms}$ ,  $C_{Lrms}$  and cylinder vibration frequency are systematically measured for  $U_r = 0.8 \sim 32$ . Furthermore,  $f_v$

behind the downstream cylinder and in the gap between the cylinders are examined.

## EXPERIMENTAL DETAILS

Measurements were conducted in a low-speed, close-circuit wind tunnel with a 2.4-m-long test section of 0.60 m  $\times$  0.60 m. Two cylinders were mounted in tandem in the horizontal mid plane of the working section. Figure 1 shows schematically experimental setup and the definitions of coordinates ( $x', y', z'$ ) and ( $x, y, z$ ), with the origins defined at the upstream and downstream cylinder centers at the mid-span, respectively; the  $x'$ - and  $x$ -axis are along the free stream direction, the  $y'$ - and  $y$ -axis are perpendicular to the  $x$ -axis in the horizontal plane and the  $z'$ - and  $z$ -axis are normal to both  $x$  and  $y$ , following the right-hand system. All cylinders were made of brass. The upstream cylinder was solid and fixed-mounted at both ends, inserting through the same diameter hole of 30 mm length at the wind tunnel walls. There was no detectable flow-induced vibration on it. On the other hand, the downstream cylinder of outer diameter  $D = 25$  mm was hollow, inner diameter 21 mm, 700 mm in length, and cantilever-mounted on an external rigid support detached from the wind-tunnel wall. To avoid further interference/complexities by cylinder free-edge vortex, an end plate was used. The free end of cylinder was just into the hole of end plates (Fig. 1a). The size of the hole on the end plate was  $2D$ , ensuring enough clearance to allow the cylinder to undergo vibrations. The active span of the cylinder, exposed in the wind tunnel is  $23.5D$  (587 mm).  $d$  was 25, 20, 15, 10 and 6 mm, respectively, and the corresponding  $d/D$  was 1.0  $\sim$  0.24, resulting in a maximum blockage of about 2.4%, and a minimum aspect ratio of 23.5.  $U_\infty$  was varied from 0.5 to 20 m/s, corresponding to variation of  $U_r$  from 0.8 to 32, Reynolds numbers ( $Re$ ) of 825 to  $3.3 \times 10^4$  based on the downstream cylinder.

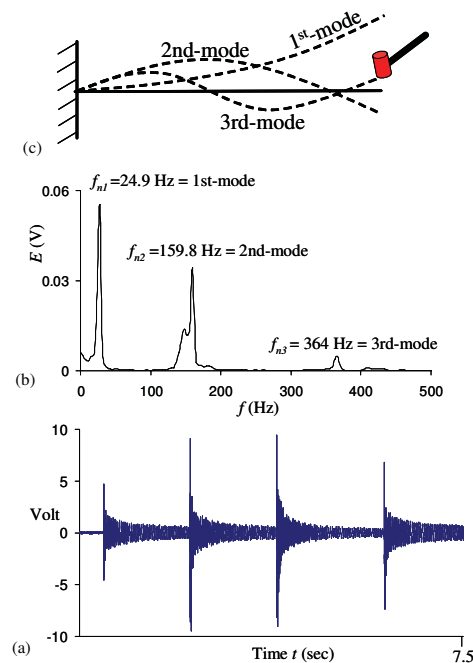


Fig. 2. (a) Signal from load cell when striking the cylinder, (b) power spectrum of the signal, and (c) modes of vibration corresponding to peaks in (b).

$m^*\zeta$  and  $f_n$  of the cylinder were obtained experimentally, providing information on structural rigidity. In order to determine  $f_n$ , the free end of the cylinder was hit slightly several times by a plastic hammer (Fig. 2c) and the signal from the load cell was captured (Fig. 2a). The gap between two successive hits was arbitrary, about 1.75 second, but should be long enough compared  $1/f_n$ . The cylinder corresponds to first, second and third modes natural frequency  $f_{n1} = 24.9$ ,  $f_{n2} = 159.8$  and  $f_{n3} = 364$  Hz, respectively (Fig. 2b). The values of  $m^*\zeta$  was obtained as 3.95. Goverdhan & Williamson (2000) surveyed the literatures available to get the information on the value of  $m^*\zeta$  examined. It was found that the researches were conducted mostly in the range of  $m^*\zeta = 0.006\sim 0.05$  and few in the range  $0.2\sim 0.8$ . The value in the present case is substantially higher than that examined previously.

Three tungsten wires of  $5\ \mu\text{m}$  in diameter and approximately 2 mm in length, one (HW1) placed at  $(x'/d, y'/d, z'/d) = (1, -1, 0)$ , and the other two (HW2 and HW2) placed at  $(x/D, y/D, z/D) = (4, 1, 0)$  and  $(4, 1, 10.55)$ , respectively (Fig. 1). They were used to measure the frequencies of vortex shedding from the cylinders.

A three-component strain-gauge load cell (KYOWA Model LSM-B-500NSA1), characterized by high response, resolution and stiffness, was installed at one end of the downstream cylinder to measure the fluid forces. Free end vibration displacement of the cylinder was measured by using a standard laser vibrometer.

A PIV system was used for flow visualization. Smoke generated from paraffin oil was released from two 1.0 mm diameter pinholes symmetrically drilled at about  $\pm 35^\circ$ , respectively, from nominal front stagnation point of the upstream cylinder. The particle images were taken using a CCD camera (HiSense type 13, 4M 8 bit, 2048x2048 pixels).

## RESULTS AND DISCUSSION

### Vibration Response

Figures 3 and 4 shows normalized vibration amplitude  $A_y/D$  and  $A_x/D$  at  $L/d = 1$  and 2. The horizontal axis  $U_r$  is based on  $f_{n1}$ , since vibration of the cylinder occurred dominantly at the first mode ( $f_{n1} = 24.9$  Hz). The figures also include the data for a single isolated cylinder ( $d/D = 0$ ). First at  $L/d = 1$ , violent vibration is unveiled at  $d/D = 0.24, 0.4, 0.6$  and  $0.8$  for  $U_r > 13, 13, 19.5$  and  $22.5$ , respectively, in addition to a visible VE at around  $U_r = 4.75$  for  $d/D = 0.24$  and  $0.4$ . For other  $d/D$ , a very tiny hump generated at the same  $U_r$  (see the insert of Fig. 3a) is the sign of VE,  $A_y/D$  at the hump is less than 0.003 corresponding to 0.075 mm vibration amplitude; hence, it can be said that VE is practically suppressed. Note that VE speed  $U_{r0}$  calculated from Strouhal number of the cylinder fixed at both ends was 5, 5.3, 5.12, 5.1, 4.74 and 4.58 for  $d/D = 0, 0.24, 0.4, 0.6, 0.8$  and  $1.0$ , respectively. It is well known that an isolated circular cylinder experiences a VE at around  $U_r = 5$ , but presently a noticeable VE is absent. This is due to fact that presently  $m^*\zeta$  is remarkably high. Bokaian & Geoola (1984a), at  $d/D = 1$  and  $L/d = 1$ , observed both VE and galloping excitation for a two dimensional model restrained to oscillate in cross-flow direction only. Their experimental conditions were  $m^*\zeta = 0.022$ ,  $U_{r0} = 6.1$  and  $Re = 600 \sim 6000$ . Vibration due to VE started at  $U_r = 4.4$  and

reached to a maximum at  $U_r = 7.54$ . On the other hand, the galloping occurred for  $U_r > 11.3$ . But presently the absence of the vibration (galloping) for  $d/D = 1$  could be attributed to either the higher value of  $m^*\zeta$  or three-dimensional model or two-degree of freedom, or combination of these. For the vibration generated cases  $d/D = 0.24 \sim 0.8$ , the starting  $U_r$  of vibration generation is lower for lower  $d/D$ , implying that a decreasing  $d/D$  anyhow causes a higher instability of flow and/or an increase of negative damping on the cylinder. Fig. 3(b) reveals that  $A_x/D$  is very small compared to  $A_y/D$ , except for  $d/D = 0.4, U_r > 20$ .

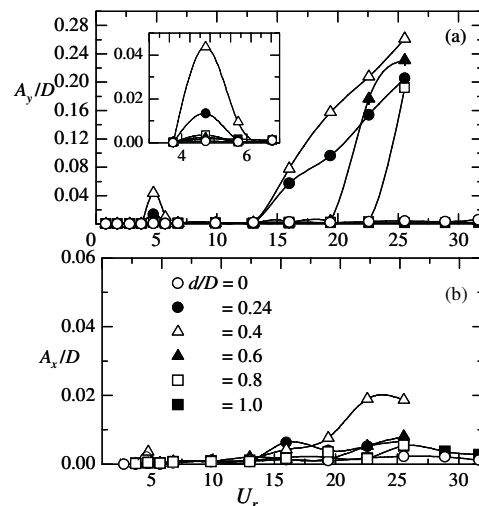


Fig. 3. Normalized vibration amplitude  $A_y/D$  and  $A_x/D$  at  $L/d = 1$ .

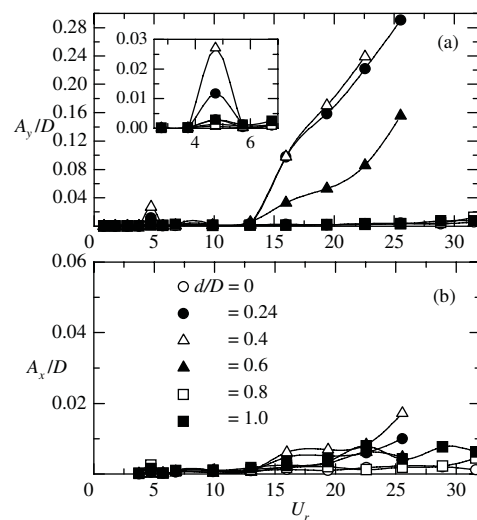


Fig. 4. Normalized vibration amplitude  $A_y/D$  and  $A_x/D$  at  $L/d = 2$ .

At  $L/d = 2$  (Fig. 4), vibration in cross-flow direction is generated at  $d/D = 0.24 \sim 0.6$  for  $U_r > 13$ , this  $d/D$  range is smaller than that at  $L/d = 1$ . Furthermore, VE is observed for  $d/D = 0.24$  and  $0.4$  and almost suppressed for other  $d/D$ . Hence it can be conferred that a cantilevered cylinder submerged in the wake of another may experience

catastrophic vibration in the cross-flow direction. In addition, a decreasing  $d/D$  is prone to generate violent vibration, which is reverse in the sense that a small cylinder placed upstream of a large cylinder may weaken forces on and vortex shedding from the large cylinder (Lesage and Gartshore 1987; Strykowski and Sreenivasan 1990).

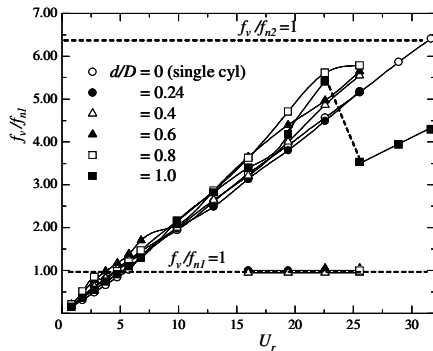


Fig. 5. Variation of  $f_v/f_{n1}$  at  $L/d = 1$ .

**Vortex Shedding**

Figure 5 shows  $f_v/f_{n1}$  at  $L/d = 1$  where  $f_v$  was obtained from power spectral analysis of HW2 signal.  $f_v/f_{n1}$  closes to 1 at about  $U_r = 4.75$ , consistent with the existent of a small peak at the same  $U_r$  in  $A_v/D-U_r$  plot (Fig. 3). At  $d/D = 0$ ,  $f_v/f_{n1}$  increases linearly and reaches  $f_v/f_{n2} = 1$  at  $U_r = 32$ .  $f_v/f_{n1}$  for other  $d/D$  also climbs monotonically except for  $d/D = 1$  which displayed a sudden drop between  $U_r = 22.6$  and  $25.5$ , marked by a dashed line. Note that  $f_v/f_{n1}$  for this  $d/D$  corresponds to Strouhal number of about 0.2 for  $U_r \leq 22.6$  ( $Re \leq 2.34 \times 10^4$ ) and 0.14 for  $U_r \geq 25.5$  ( $Re \geq 2.65 \times 10^4$ ). A deep observation made on the power spectrum results (not shown) at these two  $U_r$  explored that (i) at  $U_r = 22.6$  power spectrum of HW1 signal did not display any peak, however that of HW2 signal displayed small peak at vortex shedding frequency, and (ii) at  $U_r = 25.5$  each power spectrum of HW1 and HW2 signals displayed quite strong peak at vortex shedding frequency. These points direct that the two shear layers emanating from the upstream cylinder reattach steadily on downstream side of the downstream cylinder for  $U_r \leq 22.6$ , and those reattach alternately on the upstream side for  $U_r \geq 25.5$ . At  $d/D = 0.24, 0.4, 0.6$  and  $0.8$  for  $U_r \geq 16, 16, 19.5$  and  $22.5$ , respectively where vibration is generated, another frequency at  $f_v/f_{n1} = 1$  was observed as presented in the figure. The existence of this frequency may result from either large scale vortex shedding at  $f_{n1}$  or perturbation by the cylinder vibration. As the cylinder is cantilevered, its vibration amplitude is maximum at the free end and minimum (negligibly small) at the base; hence there should be a significant spanwise variation of vortex shedding. Typical power spectrum results of streamwise velocity at  $d/D = 0.4, L/d = 1, U_r = 19.9$  are presented in Fig. 6, showing how vortex shedding vary along the span of the cylinder and how the wake evolve along the downstream. Two peaks are observed in the power spectrum results of hotwire at the free end (Fig. 6a), corresponding to natural vortex shedding frequency and  $f_{n1}$ , respectively. While the peak at the natural vortex shedding frequency wanes as  $x/D$  increases, that at  $f_{n1}$  grows. The observation implies that, when galloping vibration is generated, the shear layers shed vortices at the natural vortex shedding frequency, and the wake significantly

oscillates at  $f_{n1}$ . Presumably the wake oscillation amplitude grows along the downstream, distorting and/or weakening the convective vortices of the natural-vortex-shedding frequency. Thus the peak heights at the natural vortex shedding frequency and  $f_{n1}$  tumble and enlarge, respectively as  $x/D$  increases. Similar observation is made in the results at the mid-span of the cylinder. At the base of the cylinder where vibration amplitude is negligible, peak at  $f_{n1}$  disappears.

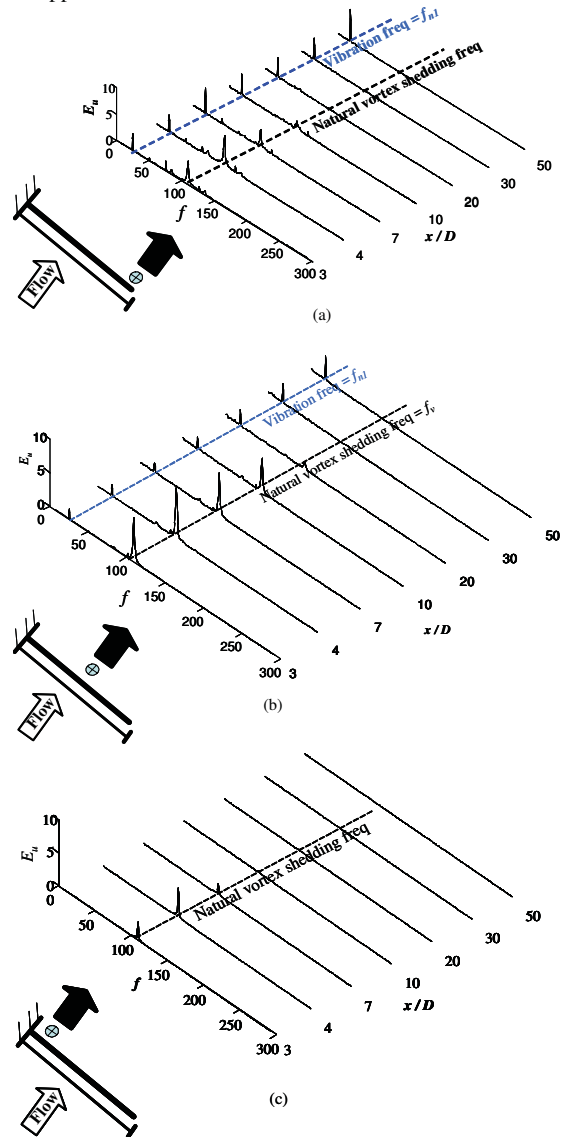


Fig. 6. Power spectrum of streamwise velocity at  $d/D = 0.4, L/d = 1, U_r = 19.9$  for hotwire at the (a) free-end ( $z/D = 10.55$ ), (b) mid-span ( $z/D = 0$ ), (c) base ( $z/D = -10.55$ ).

**Time-Mean and Fluctuating Forces**

Figure 7 shows variations of  $C_D, C_{Drms}$  and  $C_{Lrms}$  with  $U_r$  at  $L/d = 1$ .  $C_D$  for  $d/D = 0$  is about 1.22 which is close to the well-known value 1.2. Increase in  $d/D$  from 0 to 0.8 causes a reduction in  $C_D$ , by 10~13%, 14~24%, 70~75% and 90~98% for  $d/D = 0.24, 0.4, 0.6$  and  $0.8$ , respectively, the counterpart is that for  $d/D = 0$ . However, for  $d/D = 1, C_D$  is negative, about -0.45. At the same  $L/d$  and  $d/D$ , Biermann

& Herrnstein (1933), Zdravkovich & Pridden (1977) and Alam et al. (2003) observed  $C_D$  of  $-0.45$  ( $Re = 6.5 \times 10^4$ ),  $-0.53$  ( $Re = 3.1 \times 10^4$ ) and  $-0.42$  ( $Re = 6.5 \times 10^4$ ), respectively, consistent with our result. On other hand,  $C_{Drms}$  and  $C_{Lrms}$  are highly sensitive to  $U_r$  for  $d/D = 0.24 \sim 0.8$ , but less for  $d/D = 0$  and  $1.0$ . For  $d/D = 0$ , they are more or less constant at about  $0.11$  and  $0.23$ , respectively for  $U_r = 6 \sim 25$  where VE effect is absent. It could be noted that these values are the same as those measured for both ends fixed. It is interesting that though VE is practically suppressed for  $d/D \geq 0.6$  and  $d/D = 0$  at the resonance  $U_r = 4.75$  in terms of vibration amplitude (Fig. 3),  $C_{Drms}$  and  $C_{Lrms}$  amplify significantly at the  $U_r$ . They for  $d/D = 0$  however increase slightly for  $U_r > 25$ . This is due to fact that  $f_v$  is going to reach  $f_{n2}$  (Fig. 5). Note that the value of  $U_r$  corresponding to  $f_v = f_{n2}$  is  $32$ , estimated from Strouhal number. The most important feature in the figure is that  $C_{Lrms}$  for  $d/D = 0.24, 0.4, 0.6$  and  $0.8$  launches to intensify itself at  $U_r = 13, 13, 19.5$  and  $22.5$ , respectively, where vibration starts to occur. At  $U_r = 25.5$ , where  $A_y/D$  is about  $0.23, 0.26, 0.205$  and  $0.192$  for  $d/D = 0.24, 0.4, 0.6$  and  $0.8$ , respectively,  $C_{Lrms}$  intensified by  $48, 78, 57$  and  $45$  times, respectively, compared with that for  $d/D = 0$  or for a fixed cylinder.  $C_{Drms}$  is quite low even in the high-amplitude vibration regime, confirming vibration generated dominantly in the cross-flow direction. Similar observation is made at  $L/d = 2$  (Not shown).

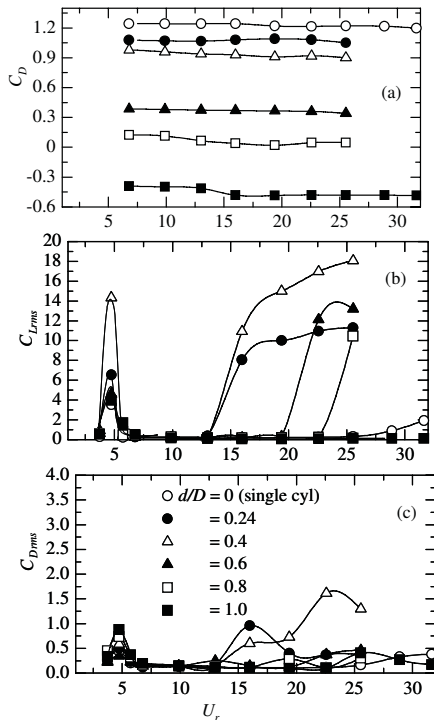


Fig. 7. Time-averaged drag ( $C_D$ ), rms lift ( $C_{Lrms}$ ) and rms drag ( $C_{Drms}$ ) forces at  $L/d = 1$ .

**Vibration Generation Mechanism**

Galloping vibration is caused by a non-linear coupling between the wake and the structural vibrations. A cross-wind oscillation of the structure periodically changes the attack angle of the relative flow velocity. This variation in the attack angle produces variation in the aerodynamic

forces on the structure, and hence produces vibration of the structure. According to quasi-steady theory of galloping (Den Hartog 1956; Blevins 1990), a circular cylinder in general is not susceptible to galloping, because it is always symmetric with respect to a flow at any attack angle. If it is, however, placed in a non-uniform flow, like the flow in a wake, it may not be symmetric with respect to the flow approaching on. Two tandem circular cylinders in the reattachment regime may experience galloping due to two reasons: firstly the two cylinders behave like a combined body which is not symmetric with respect to flow at all attack angles; secondly the downstream cylinder is submerged in a non-uniform flow.

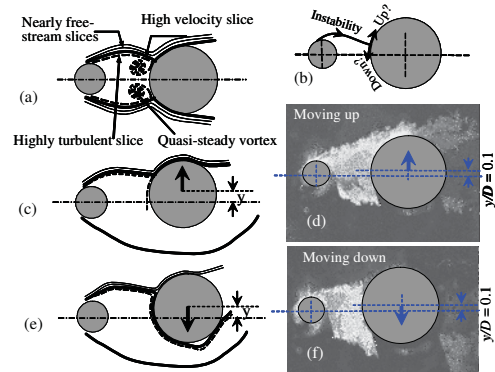


Fig. 8. Flow structure generating galloping. (a) No vibration: steady-reattachment flow. (b) Instability generation. For a given displacement, visualized flow ( $d/D = 0.4, L/d = 2, U_r = 19.9$ ) and sketch when cylinder moving (c, d) upward, (e, f) downward..

When both cylinders are fixed (Fig. 8a), the two shear layers emanating from the upstream cylinder reattach steadily on the downstream cylinder. The thickness of a shear layer can be divided into three slices: highly turbulent slice, high velocity slice and nearly free-stream slice. Vibration for two tandem cylinders mainly results from the switching instability of the shear layers originated from the upstream cylinder, as sketched in Fig. 8(b). The switching instability is generated from whether the high velocity slice of a shear layer passes on the same side (up?) or opposite side (down?) of the downstream cylinder. The high velocity slice generates highly negative pressure on the surface over which it goes (Alam et al. 2005). Now let us discuss the physics of flow on the vibrating cylinder. When the cylinder is moving upward from its centerline (Figs. 8c, d), the high velocity slice of the upper shear layer goes on the upper side and causes an upward lift force to pull the cylinder upward. On the other hand, when the cylinder is moving down (Figs. 8e, f), toward the centerline, the high velocity slice of the same shear layer sweeps the lower side; hence a downward lift force is generated to pull the cylinder toward the centerline. Details of flow structure in half of a period are given in Fig. 9. Similarly, the next half cycle is associated with the lower shear layer. The vibration may be termed as shear-layer-reattachment-induced vibration. Previous sections proved that a smaller  $d/D$  is more prone to generate vibration. Why? As  $d/D$  tends to be small, the upstream cylinder wake narrows, and the shear-layer reattachment position on the downstream cylinder moves to the front stagnation point. Hence the shear layer is more prone to switch and results in the vibration. If the upstream cylinder is larger than or equal to the downstream one, i.e.,  $d/D \geq 1$ , the upstream wake becomes wider, and the shear layers get

enough stability to pass over the respective side of the downstream cylinder, hence no vibration is generated. Lam and To (2003) performed experimental investigation for  $d/D = 2$  and observed no vibration.

## CONCLUSIONS

Flow-induced forces, vibration characteristics and vortex shedding frequency of a cantilevered circular cylinder in the presence of an upstream cylinder of various diameters are investigated with  $L/d = 1$  and 2 and  $d/D = 1 \sim 0.24$ . The cylinder system had a high value of  $m^*\zeta = 3.95$ . The preliminary investigation leads to following conclusions.

- (i) Vortex-excited vibration occurs for  $d/D = 0.24$  and 0.4 at resonance  $U_r \approx 4.75$  and is suppressed for  $d/D \geq 0.6$  and  $d/D = 0$ . In addition, a violent divergent lateral structural vibration is observed at  $d/D = 0.24 \sim 0.8$  for  $L/d = 1$  and at  $d/D = 0.24 \sim 0.6$  for  $L/d = 2$ . The smaller  $d/D$ , the narrower is the wake in the gap of the cylinders and the lower is  $U_r$  at which the violent vibration occurs. For example, this  $U_r$  is 13, 13, 19.5 and 22.5 for  $d/D = 0.24, 0.4, 0.6$  and 0.8, respectively, for  $L/d = 1$ .

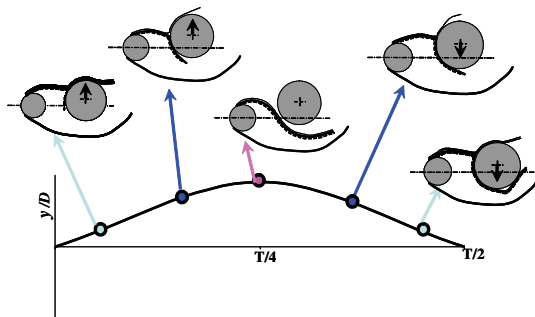


Fig. 9. Change of flow structure during cylinder oscillation in a half period.

- (ii) While  $C_D$  is almost independent of the cylinder vibration,  $C_{Drms}$  and  $C_{Lrms}$  are amplified drastically. For example, at  $U_r = 25.5$ , where  $A_y/D$  is about 0.23, 0.26, 0.205 and 0.192 for  $d/D = 0.24, 0.4, 0.6$  and 0.8, respectively,  $C_{Lrms}$  grows by 48, 78, 57 and 45 times, respectively, compared with that of  $d/D = 0$  or a stationary cylinder. Meanwhile,  $C_D$  remains unchanged. At the resonance  $U_r$ ,  $C_{Drms}$  and  $C_{Lrms}$  are amplified significantly, regardless of whether the cylinder is vibrating or not.
- (iii) Two predominant frequencies in the wake were identified, associated with natural vortex shedding and the vibration of the cylinder, respectively. While the vortices associated with the natural vortex shedding frequency decay rapidly, those associated with the vibration frequency persist in the downstream.
- (iv) The possible mechanism of the violent vibration is that the upstream cylinder wake narrows with decreasing  $d/D$ , and the shear-layer reattachment position on the downstream cylinder approaches the forward stagnation point. As a result, the high-speed slice of the shear layer could impinge upon alternately on the two sides of the cylinder, thus getting it excited.

## ACKNOWLEDGEMENT

The authors wish to acknowledge support given to them by the Research Grants Council of HKSAR through Grant PolyU 5334/06E.

## REFERENCES

- Alam, M.M, Moriya, M., Takai, K., and Sakamoto, H., 2003, "Fluctuating Fluid Forces Acting on Two Circular Cylinders in a Tandem Arrangement at a Subcritical Reynolds Number", *Journal of Wind Engineering and Industrial Aerodynamics*, Vol. 91, pp. 139-154.
- Alam, M. M., Sakamoto H., and Zhou, Y., 2005, "Determination of Flow Configurations and Fluid Forces acting on Two Staggered Circular Cylinders of Equal Diameter in Cross-Flow", *Journal of Fluids Structures*, Vol. 21, pp. 363-394.
- Biermann, D. and Herrnstein, Jr., 1933, "The Interference between Struts in Various Combinations", *National Advisory Committee for Aeronautics*, Tech. Rep. 468.
- Blevins, R.D., 1990, "Flow-Induced Vibrations", second ed. Van Nostrand Reinhold, New York.
- Bokaian, A., and Geoola, F., 1984b, "Proximity-Induced Galloping of Two Interfering Circular Cylinders", *Journal of Fluid Mechanics*, Vol. 146, pp. 417-449.
- Bokaian, A. and Geoola, F., 1984a, "Wake-Induced Galloping of Two Interfering Circular Cylinders. *Journal of Fluid Mechanics*, Vol. 146, pp. 383-415.
- Brika, D. and Laneville, A., 1997, "Vortex-Induced Oscillations of Two Flexible Circular Cylinders Coupled Mechanically", *Journal of Wind Engineering and Industrial Aerodynamics*, Vol. 69-71, pp. 293-302.
- Brika, D., and Laneville, A., 1999, "The Flow Interaction between a Stationary Cylinder and a Downstream Flexible Cylinder", *Journal of Fluids Structures*, Vol. 13, pp. 579-606.
- Den Hartog, J.P., 1956, "Mechanical Vibrations", forth ed. McGraw-Hill, New York.
- Govardan, R., and Williamson, C. H. K., 2000, "Modes of Vortex Formation and Frequency Response of a Freely Vibrating Cylinder", *Journal of Fluid Mechanics*, Vol. 420, pp. 85-130.
- Hover, F.S., and Triantafyllou, M.S., 2001, "Galloping Response of a Cylinder with Upstream Wake Interference", *Journal of Fluids Structures*, Vol. 15, pp. 503-512.
- Lam, K.M., and To, A.P., 2003, "Interference Effect of an Upstream Larger Cylinder on the Lock-in Vibration of a Flexibly Mounted Circular Cylinder", *Journal of Fluids Structures*, Vol. 17, pp. 1059-1078.
- Lesage, F., and Gartshore, I.S., 1987, "A Method of Reducing Drag and Fluctuating Side Force on Bluff Bodies", *Journal of Wind Engineering and Industrial Aerodynamics*, Vol. 25, pp. 229-245.
- Mahir, N., and Rockwell, D., 1996, "Vortex Formation from a Forced System of Two Cylinders, Part I: Tandem Arrangement", *Journal of Fluids Structures*, Vol. 10, pp. 473-490.
- Strykowski, P. J., and Sreenivasan, K. R., 1990, "On the Formation and Suppression of Vortex Shedding at Low Reynolds Numbers", *Journal of Fluid Mechanics*, Vol. 218, pp. 71-107.
- Zdravkovich, M. M., and Pridden, D.L., 1977, "Interference between Two Circular Cylinders; Series of Unexpected Discontinuities", *Journal of Wind Engineering and Industrial Aerodynamics*, Vol. 2, pp. 255-270.